

Nonequilibrium Phase Transitions and Nonequilibrium Critical Point from AdS/CFT

Shin Nakamura*

Department of Physics, Kyoto University, Kyoto 606-8502, Japan

We find novel phase transitions and critical phenomena that occur only outside the linear-response regime of current-driven nonequilibrium states. We consider a $(3+1)$ -dimensional system of strongly-interacting quantum gauge theory defined at the microscopic level. We compute its nonlinear non-ballistic conductivity by using the AdS/CFT correspondence. We find that the system exhibits a nonequilibrium first-order phase transition where the conductivity jumps discontinuously at finite current density. The sign of the differential conductivity also changes there. A nonequilibrium critical point is found at the end point of the first-order regime where critical phenomena are observed. We define nonequilibrium analogues of critical exponents, and their numerical values are obtained. In light of the possible universality, we expect that the newly discovered nonequilibrium critical point can also be found in nature: this provides a prediction of superstring theory for the real world. We also propose a nonequilibrium-steady-state analogue of thermodynamic potential in terms of the gravity-dual theory.

PACS numbers: 05.70.Ln, 11.25.Tq, 05.70.Jk

Introduction.— Nonequilibrium physics is one of the central subjects in modern physics. Although the linear response theory provides a computational framework of the transport coefficients at the vicinity of thermal equilibrium, its extension to the nonlinear regime is still a great challenge. A key question in nonequilibrium physics is how to extract the macroscopic physics from the underlying microscopic theories when the systems are out of equilibrium.

Recently, a great deal of attention has been paid to the Anti-de Sitter space (AdS)/Conformal Field Theory (CFT) correspondence [1, 2]. The AdS/CFT correspondence is essentially a map between a microscopic theory of strongly-interacting quantum gauge theory and a classical gravity: it is capable of describing the microscopic physics. However, an interesting feature of this correspondence is emergence of the macroscopic physics in the gravity side. For example, a plasma of gauge particles is mapped to a black hole geometry [3] that has a notion of temperature given by the Hawking temperature. The point is that the coarse graining of the gauge theory is accomplished in the gravity side just by solving the classical equations of motion. This simplification tempts us to apply AdS/CFT to many-body physics out of equilibrium.

In this Letter, we study nonequilibrium phase transitions by using the AdS/CFT correspondence. Our system is a strongly-interacting gauge-theory plasma driven to far from equilibrium by a constant current: a current-driven nonequilibrium steady state (NESS). We discover novel nonequilibrium phase transitions and nonequilibrium critical point in this system. Usually, a drawback of AdS/CFT is that we need to deal with an idealized gauge theory that is not exactly realized in nature at the microscopic level, in order to ensure the correspondence well-defined. However, our aim is to study the macroscopic properties of NESS that may be shared by wide range of systems regardless of the details of each microscopic theory. In light of the possible universality, we expect that the nonequilibrium critical point we find can be observed in nature as well: the present work makes a prediction of superstring theory for the real world.

Our phase transitions are associated with the nonlinear con-

ductivity of the system. It has been found in [4] that the gauge-theory plasma, that will be defined in detail later, exhibits negative differential conductivity (NDC) in the low-current-density region that is categorized into the S-shaped NDC (SNDC) in [5]. Here, the differential conductivity is defined as $\partial J/\partial E$ where J and E are the current density and the external electric field acting on the charge carriers, respectively. The difference from the conventional conductivity $\sigma = J/E$ is that the differential conductivity can be either negative or positive whereas σ cannot be negative. In fact, SNDC has been experimentally observed in various current-driven systems [5] including those of strongly-correlated electrons (see, e.g., [6]). It has been found in [4] that the NDC turns to positive differential conductivity (PDC) in the high-current-density region. The transition between them observed in [4] is smooth: it is a crossover.

In this Letter, we further survey how the differential conductivity depends on the parameters of the system such as the current density J and the temperature T of the heat bath. Here, we do not request the presence of the notion of temperature for the charge carriers since they are out of equilibrium. However, we still have a definite temperature in the heat bath attached to the system of the charge carriers. The temperature we control is that of the heat bath. In the high-temperature region, we find that the crossover moves to a first-order transition where both σ and the differential conductivity discontinuously jump. We also find a critical point at the end point of the first-order line on the phase diagram. The differential conductivity still changes discontinuously but σ varies continuously at the critical point. We shall define the NESS analogues of the critical exponents and compute them later. Since the analysis in the gravity dual is essentially based on the classical mechanics, the gravity dual naturally provides a NESS analogue of thermodynamic potential: we propose a generalization of the thermodynamic potential to NESS. As far as the author knows, these types of current-driven nonequilibrium phase transitions and critical point have been reported neither experimentally nor theoretically so far.

Microscopic theory.— We choose our microscopic theory

by asking how much its AdS/CFT dual is established, rather than asking whether the microscopic details are realized in nature, since we are interested in only the macroscopic properties of NESS that may be independent of the microscopic details. One of the gauge theories whose AdS/CFT dual is well-established is the $(3 + 1)$ -dimensional strongly-coupled $SU(N_c)$ $\mathcal{N} = 4$ super-symmetric Yang-Mills theory ($\mathcal{N} = 4$ SYM) at the large- N_c limit with a single flavor of fundamental $\mathcal{N} = 2$ hypermultiplet. This is a supersymmetric cousin of Quantum Chromodynamics (QCD), but its supersymmetry is broken at finite temperatures. This gauge theory is a conformal field theory at the large- N_c limit. However, since several dimensional parameters (such as T , J , and the mass of the charge carriers) are switched on, the physical quantities are still non-trivial functions of T and J in general. We employ this theory as our microscopic theory.

The $\mathcal{N} = 4$ SYM sector (gluon sector) contains the gauge particles in the adjoint representation, which we call “gluons” in this Letter. The $\mathcal{N} = 2$ hypermultiplet sector (quark sector) contains the particles in the fundamental representation and in the anti-fundamental representation. We call these particles “quarks” and “antiquarks,” respectively. The quark (antiquark) carries a unit positive (negative) quark charge. They play a role of, for example, electrons and holes in condensed matters: the charge carriers. The interaction among them is mediated by the gluons: the gluons play a role of phonons, for example.

We consider the conductivity associated with the quark charge, and it is the quark-charge current that drives our system out of equilibrium. NESS is realized in the following way [7]. We take the large- N_c limit that makes the degree of freedom (DOE) of the gluon sector (which is $O(N_c^2)$) sufficiently larger than that of the quark sector (which is $O(N_c)$). We also make the gluon sector equilibrium at definite temperature T . The interaction between the gluon sector and the quarks sector generates the dissipation in the presence of the quark current: the gluons absorb the momentum and the energy of the charge carriers. Because of the large DOE, the heat capacity of the gluon sector is large enough so that the temperature of the gluon sector is well-approximated as a constant. The gluon sector plays a role of heat bath, and NESS of the quark sector is realized by making the dissipation into the heat bath and the work of the external field in balance.

Let us specify the conditions we impose on the system. We consider neutral systems where the total quark-charge density is zero. This means that the finite current is realized by the equal numbers of the quarks and the antiquarks flowing in the opposite directions. We assume that the system is steady and homogeneous. We also assume that the system has infinitely large volume: we are *not* dealing with mesoscopic systems. We consider current-driven systems where J (the quark-charge current density) is a control parameter. In this sense, E , the external field acting on the quark charge, is a quantity obtained by the measurement at given J . We choose the direction of the electric field (and hence that of the current) in the x direction. We employ the natural units $c = \hbar = k_B = 1$.

Nonlinear conductivity in AdS/CFT.— The gravity dual of the foregoing microscopic theory is the so-called D3-D7 system [8]. The computational technique of the nonlinear conductivity has been proposed in [9] in the framework of the AdS/CFT correspondence, and we follow it. Let us briefly sketch the idea of [9] to define our notation.

The gluon sector at finite temperature is mapped to the gravity theory on a curved geometry which is a direct product of a 5-dimensional AdS-Schwarzschild black hole (AdS-BH) and S^5 [3]. The metric of the AdS-BH part is given by [19]

$$ds^2 = -\frac{1}{z^2} \frac{(1 - z^4/z_H^4)^2}{1 + z^4/z_H^4} dt^2 + \frac{1 + z^4/z_H^4}{z^2} dx^2 + \frac{dz^2}{z^2}, \quad (1)$$

where z ($0 \leq z \leq z_H$) is the radial coordinate of the black hole geometry. The AdS-BH has a horizon at $z = z_H$ and a boundary at $z = 0$. The Hawking temperature, that corresponds to the temperature of the gluon sector (hence that of the heat bath), is given by $T = \sqrt{2}/(\pi z_H)$. \vec{x} and t denote the $(3 + 1)$ -dimensional spacetime coordinates on which the gauge theory is defined. The metric of the S^5 part is given by $d\Omega_5^2 = d\theta^2 + \sin^2 \theta d\psi^2 + \cos^2 \theta d\Omega_3^2$, where $0 \leq \theta \leq \pi/2$, and $d\Omega_d$ is the volume element of the unit d -dimensional sphere. The radius of the S^5 has been taken to be 1, for simplicity. This is equivalent to choose the 't Hooft coupling λ of the gauge theory at $\lambda = (2\pi)^2/2$.

The quark sector is mapped to a D7-brane [10] embedded to the above geometry. The 3-dimensional part of the D7-brane is wrapped on the S^3 part in the S^5 , the radius of which is given by $\cos \theta$: the configuration of the D7-brane is specified by the function $\theta(z)$ [8]. We employ the probe approximation where the backreaction of the D7-brane to the AdS-BH is neglected. This is justified at the large- N_c limit, and is consistent with the picture to regard the AdS-BH as the heat bath. The behavior of $\theta(z)$ at the vicinity of the boundary $z = 0$ is related to the current quark mass m_q [8] as $\theta(z) = m_q z + \frac{1}{2} [(\bar{q}q)/N + m_q^2/3] z^3 + O(z^5)$. Here, $(\bar{q}q)$ denotes the chiral condensate [20]. Throughout the analysis, we fix m_q at a designed value. There is a $U(1)$ gauge field A_μ on the D7-brane. E and J are related to A_x through $A_x(z, t) = -Et + \text{const.} + J(2N)^{-1} z^2 + O(z^4)$, where $N = N_c/(2\pi)^2$ in our convention and we have employed the gauge $\partial_x A_t = 0$ [9]. The dynamics of $\theta(z)$ and $A_x(z, t)$ is governed by the D7-brane action, $S_{D7} = \int dt d^3x dz \mathcal{L}_{D7}$, where \mathcal{L}_{D7} is explicitly written as $\mathcal{L}_{D7} = -N \cos^3 \theta \sqrt{|g_{tt}| g_{xx} g_{zz} - g_{zz} (\dot{A}_x)^2 + |g_{tt}| (A'_x)^2}$ [9]. Here, the prime (the dot) denotes the differentiation with respect to z (t). g_{tt} , g_{xx} and g_{zz} are the components of the induced metric on the D7-brane, and they are equal to those of the background metric (1) except for $g_{zz} = 1/z^2 + \theta'(z)^2$. If we regard z as a “time coordinate,” $J = \partial \mathcal{L}_{D7} / \partial A'_x$ is a conserved “canonical momentum” since \mathcal{L}_{D7} does not contain A_x explicitly. Then it is convenient to introduce a “Routhian” $\tilde{\mathcal{L}}_{D7} = \mathcal{L}_{D7} - A'_x \partial \mathcal{L}_{D7} / \partial A'_x$ [11, 12] which is given in terms of A_x , J , θ and θ' [9]:

$$\tilde{\mathcal{L}}_{D7} = -\sqrt{g_{zz}(g_{xx} - \dot{A}_x^2/|g_{tt}|)(N|g_{tt}|g_{xx}^2 \cos^6 \theta - J^2)}. \quad (2)$$

The Euler-Lagrange equation from (2) determines $\theta(z)$ under given $E = -\dot{A}_x$ and J . The relationship between E and J is determined by requesting the on-shell D7-brane action to be real-valued: the inside of the square root in (2) has to be positive semidefinite [9]. This condition yields $\sigma = NT(e^2 + 1)^{1/4} \cos^3 \theta(z_*)$, where $z_* = [\sqrt{e^2 + 1} - e]^{1/2} z_H$ and $e = 2E/(\pi\sqrt{2\lambda T^2})$ [9]. $z = z_*$ is the location where the inside of the square root in (2) touches zero [9].

We need numerical analysis to obtain $\theta(z_*)$ explicitly. The boundary conditions we employ are $\theta(z)/z|_{z=0} = m_q$ and $\theta'|_{z=z_*} = [B - \sqrt{B^2 + C^2}]/(Cz_*)$. Here $B = 3z_H^8 + 2z_H^4 z_*^4 + 3z_*^8$ and $C = 3(z_*^8 - z_H^8) \tan \theta(z_*)$. The condition for $\theta'|_{z=z_*}$ comes from the EOM at $z = z_*$ [4, 13] with the assumption $\theta(z_*) \neq \pi/2$. Notice that $\theta'|_{z=z_*}$ is given in terms of T, J, E and N_c . Let us fix $N_c = 40$ for numerical computation. After the solution $\theta(z)$ is obtained, we estimate m_q from $\theta(z)/z|_{z=0}$: we obtain m_q as a function of T, J and E . We choose E (under given T and J) so that m_q agrees with the designed value. Since the numerical analysis becomes unstable at $z = 0, z = z_*$ and at $z = z_H$, we avoid these points by introducing small cutoffs in the numerical computations.

Nonequilibrium phase transitions.— Let us fix $m_q = 1$. The J - E characteristics at various T are shown in Fig. 1. The system exhibits NDC in the small- J region whereas PDC in the large- J region. The NDC region is smoothly connected to the PDC region for $T < T_c$, showing a crossover at point A. However, the curve for $T > T_c$ has an intermediate region (between points D and G) where three values of E are possible at a given J . In terms of the D7-brane dynamics, we have three different solutions to the equations of motion of $\theta(z)$. If we start in the small- J region, E has to jump to the lower value at somewhere in the intermediate region, and then PDC appears. Since E (hence σ) changes discontinuously, we call it first-order transition. The boundary between the crossover regime and the first-order regime is found at $T = 3.4365 \times 10^{-1} = T_c$. The differential resistivity $\partial E/\partial J$ diverges at $J = 1.86 \times 10^{-2} = J_c$ (indicated by B) although σ changes continuously. We call this transition at $(T, J) = (T_c, J_c)$ second-order transition. The minimum value of E for each curve is the critical electric field for insulation breaking. The system is an insulator at sufficiently low E , but the strong enough external field makes pair creations of the quarks and the antiquarks which can carry the current [9][21].

An immediate question is how to determine the transition point in the intermediate region. In equilibrium systems, the stable phase is the phase of minimum thermodynamic potential (TP), and the transition point is defined as the point where the two phases share a common TP. However, generalization of the idea of TP into nonequilibrium cases has not been completely established. Interestingly, we can determine the most stable phase by considering the Hamiltonian of the D7-brane in the present case. The question is which D7-brane configuration is most stable among the three possible solutions. Since the dynamics of the D7-brane in the dual picture is governed

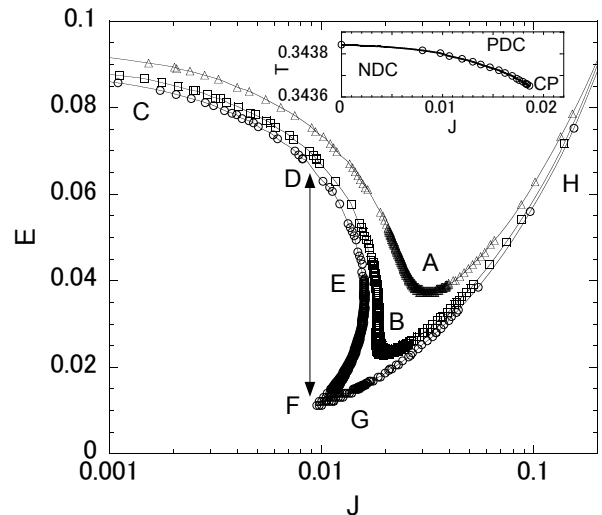


FIG. 1: The J - E curves at $T = 3.4379 \times 10^{-1} > T_c$ (circle), $T = 3.4365 \times 10^{-1} = T_c$ (box), and $T = 3.4337 \times 10^{-1} < T_c$ (triangle). Inset: the phase diagram. CP denotes the critical point.

by the classical mechanics, the most stable configuration is that of the smallest Hamiltonian. We have seen that the D7-brane dynamics is governed by $\tilde{\mathcal{L}}_{D7}$. Therefore, let us construct the Hamiltonian density $\tilde{\mathcal{H}}_{D7} = \dot{A}_x \partial \tilde{\mathcal{L}}_{D7} / \partial \dot{A}_x - \tilde{\mathcal{L}}_{D7}$, which is explicitly given by

$$\tilde{\mathcal{H}}_{D7} = g_{xx} \sqrt{|g_{tt} g_{zz}|} \sqrt{\frac{N^2 \cos^6 \theta |g_{tt} g_{xx}^2 - J^2}{|g_{tt} g_{xx} - E^2|}}. \quad (3)$$

Note that $\tilde{\mathcal{H}}_{D7}$ is *regular* at the horizon (where $g_{tt} = 0$). The divergence at the horizon (which corresponds to the IR divergence in the gauge theory) in $\tilde{\mathcal{L}}_{D7}$ is canceled by that in $\dot{A}_x \partial \tilde{\mathcal{L}}_{D7} / \partial \dot{A}_x$ within the Legendre transformation. We propose to define the thermodynamic potential per unit 3d volume in our system by

$$\tilde{H}_{D7}(T, J; m_q) = \lim_{\epsilon \rightarrow 0} \left[\int_{\epsilon}^{z_H} dz \tilde{\mathcal{H}}_{D7} - L_{\text{count}} \right], \quad (4)$$

where L_{count} denotes the counter terms that renormalize the divergence at the boundary $z = 0$ (which corresponds to the UV divergence in the gauge theory). L_{count} is given by $L_{\text{count}} = L_1 + L_2 - L_F + L_f$, where L_1, L_2, L_F , and L_f are explicitly given in [9, 15]. The relative sign between L_F and the others has to be flipped comparing to the counter terms for the action owing to the Legendre transformation.

It is found from the numerical analysis that the configurations between F and G have the smallest \tilde{H}_{D7} comparing to those between E and F, and those between D and E at a given J . Therefore, the transition between NDC and PDC occurs at D and F as is indicated by the arrow in Fig. 1.[22] Notice that the Maxwell construction does not apply since J and E are not conjugate to each other.

The next question is how to define the critical exponents. We find that the NDC phase and the PDC phase are connected via the crossover region on the phase diagram (shown in the inset of Fig. 1): the symmetry of the system does not change through the transition. This resembles the liquid-gas transitions and the Mott insulator-to-metal transitions in equilibrium systems, whose critical points are in the same universality class of the Ising model [16]. In the liquid-gas transitions, the critical exponents β and δ are given by $\Delta\rho \propto |T - T_c|^\beta$ along the first-order-transition line and $|\rho - \rho_c| \propto |P - P_c|^{1/\delta}$ along the $T = T_c$ line. Here, ρ and P are the density and the pressure, respectively, and ρ_c and P_c are their critical values. $\Delta\rho$ is the difference of the density between the liquid phase and the gas phase. In the equilibrium Mott insulator-to-metal transitions, the critical exponents can be detected by using the conductivity instead of the density [16, 17]. Therefore, let us generalize the definition of the exponent β into the nonequilibrium cases as $\Delta\sigma \propto |T - T_c|^\beta$ where the temperature is that of the heat bath and $\Delta\sigma$ is the difference of the conductivity between the NDC phase and the PDC phase along the first-order-transition line. We regard $\Delta\sigma$ as a probe of the order parameter. The pressure of the system is not a control parameter within the present setup, but we have J instead. Let us define a new critical exponent $\tilde{\delta}$ by $|\sigma - \sigma_c| \propto |J - J_c|^{1/\tilde{\delta}}$ along the $T = T_c$ line.

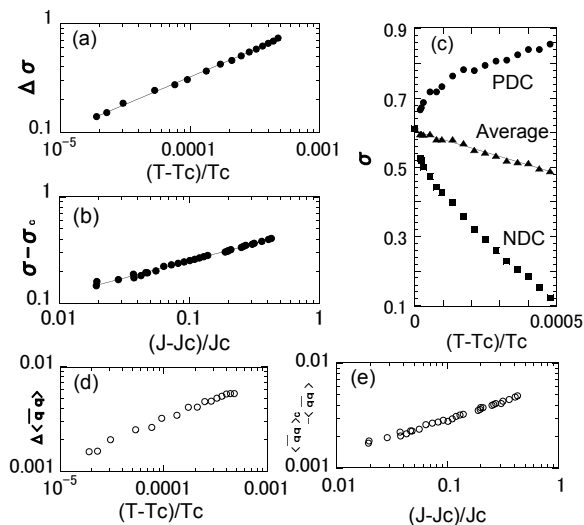


FIG. 2: Critical behaviors of various quantities. (a): $\Delta\sigma$, (b): $\sigma - \sigma_c$, (c): conductivities and the average, (d): $\Delta\langle\bar{q}q\rangle$, and (e): $\langle\bar{q}q\rangle_c - \langle\bar{q}q\rangle$.

The behaviors of the conductivity are plotted in Fig. 2 (a) and in Fig. 2 (b). Critical phenomena with $\beta = 0.52 \pm 0.03$ and $\tilde{\delta} = 3.1 \pm 0.2$ are found. The conductivities in the two phases and their average, along the first-order-transition line, are shown in Fig. 2 (c). They resemble of the coexistence line and the law of rectilinear diameter in the liquid-gas transitions: the average conductivity shows a linear behavior within the numerical error. In Fig. 2 (d) and in Fig. 2 (e), the behaviors of the chiral condensate are shown. The

chiral condensate is more sensitive to the possible numerical errors since it is read by $\partial_z^3\theta|_{z=0}$: we need further analysis to estimate the precise values of the exponents. Currently, we observe preliminary values of the exponents $\beta_{\text{chiral}} \sim 0.4$ and $\tilde{\delta}_{\text{chiral}} \sim 3$, where we have defined the exponents by $\Delta\langle\bar{q}q\rangle \propto |T - T_c|^{\beta_{\text{chiral}}}$ along the first-order-transition line and by $|\langle\bar{q}q\rangle - \langle\bar{q}q\rangle_c| \propto |J - J_c|^{1/\tilde{\delta}_{\text{chiral}}}$ along the $T = T_c$ line. Here, $\Delta\langle\bar{q}q\rangle$ is the difference of $\langle\bar{q}q\rangle$ between the two phases and $\langle\bar{q}q\rangle_c$ is the chiral condensate at the critical point.

The features similar to the equilibrium phase transitions and the picture of classical mechanics in the gravity dual suggest that it may be possible to construct a phenomenological model of our nonequilibrium phase transitions similar to the Landau theory. It is also suggestive that the steady state thermodynamics [18] may work in our nonequilibrium systems. In light of the universality, we expect that the same nonequilibrium critical point in the current-driven systems can be experimentally found in real materials.

Acknowledgements: The author thanks H. Fujii, H. Hayakawa, S. Inutsuka, T. Iritani, H. Kawai, Y. Hikida, S. Kinoshita, C. Maes, Y. Minami, S. Mukohyama, T. Oka, R. Sakano, S. Sasa, A. Shimizu, H. Suganuma, T. Takayanagi and H. Tasaki for useful comments. Discussions during the YITP conferences YITP-W-11-11, YITP-W-11-14, YITP-W-11-16, YITP-T-11-05 at the Yukawa Institute for Theoretical Physics at Kyoto University, the conferences KEK-TH2012, QMKEK4 at the High Energy Accelerator Research Organization (KEK), GCOE symposium 2010, GCOE symposium 2011 at Kyoto University, and the conference QHEC11 at Keio University, were useful. This work was supported in part by the Grant-in-Aid (GIA) for Scientific Research on Innovative Areas No. 2104, and GIA for Challenging Exploratory Research # 23654132.

* E-mail: nakamura@ruby.scphys.kyoto-u.ac.jp

- [1] J. M. Maldacena, *Adv. Theor. Math. Phys.* **2**, 231 (1998); [*Int. J. Theor. Phys.* **38**, 1113 (1999)].
- [2] S. S. Gubser, I. R. Klebanov and A. M. Polyakov, *Phys. Lett. B* **428**, 105 (1998); E. Witten, *Adv. Theor. Math. Phys.* **2**, 253 (1998).
- [3] E. Witten, *Adv. Theor. Math. Phys.* **2**, 505 (1998).
- [4] S. Nakamura, *Prog. Theor. Phys.* **124**, 1105 (2010).
- [5] E. Schöll, *Nonlinear Spatio-Temporal Dynamics and Chaos in Semiconductors* (Cambridge Univ. Press, Cambridge 2001).
- [6] T. Oka and H. Aoki, *Lect. Notes Phys.* **762**, 251 (2009).
- [7] A. Karch, A. O'Bannon and E. Thompson, *JHEP* **0904**, 021 (2009).
- [8] A. Karch and E. Katz, *JHEP* **0206**, 043 (2002).
- [9] A. Karch and A. O'Bannon, *JHEP* **0709**, 024 (2007).
- [10] For D-branes and superstring theory, see e.g., J. Polchinski, *String theory. Vol. 1, Vol. 2*, (Cambridge Univ. Press, Cambridge 1998).
- [11] S. Nakamura, Y. Seo, S. J. Sin and K. P. Yogendran, *J. Korean Phys. Soc.* **52**, 1734 (2008).
- [12] S. Kobayashi, D. Mateos, S. Matsuura, R. C. Myers and R. M. Thomson, *JHEP* **0702**, 016 (2007).

- [13] T. Albash, V. G. Filev, C. V. Johnson and A. Kundu, JHEP **0808**, 092 (2008).
- [14] J. Erdmenger, R. Meyer and J. P. Shock, JHEP **0712**, 091 (2007).
- [15] A. Karch, A. O'Bannon and K. Skenderis, JHEP **0604**, 015 (2006).
- [16] See, e.g., S. Papanikolaou et al., Phys. Rev. Lett. **100**, 026408 (2008), and references therein.
- [17] See, e.g., P. Limelette et al., Science **302**, 89 (2003); F. Kagawa, K. Miyagawa and K. Kanoda, Nature **436**, 534 (2005).
- [18] See, e.g., Y. Oono and M. Paniconi, Prog. Theor. Phys. Suppl. **130**, 29 (1998).
- [19] We have taken the string tension to be 1 for simplicity.
- [20] The exact operator for the present model is written in [12].
- [21] See also [13, 14], for earliest works on the insulator-conductor transitions in the present model.
- [22] We expect that hysteresis $F \rightarrow D$ and $E \rightarrow G$ may also occur.